ELSEVIER

Marine Geology 184 (2002) 41–60

MARINE GEOLOGY
INTERNATIONAL JOURNAL OF MARINE GEOLOGY, GEOCHEMISTRY AND GEOPHYSICS

www.elsevier.com/locate/margeo

The July 1996 flood deposit in the Saguenay Fjord, Quebec, Canada: implications for sources of spatial and temporal backscatter variations

Roger Urgeles [a,b,*], Jacques Locat [a], Thierry Schmitt [a], John E. Hughes Clarke [c]

[a] *Département de géologie et de génie géologique, Université Laval, Pavillon Pouliot, Ste-Foy, QC, Canada G1K 7P4*
[b] *Departament d'Estratigrafia i Paleontologia, Universitat de Barcelona, Campus de Pedralbes, 08071 Barcelona, Catalonia, Spain*
[c] *Ocean Mapping Group, Department of Geodesy and Geomatics Engineering, University of New Brunswick, Fredericton, NB, Canada E3B 5A3*

Received 19 March 2001; accepted 4 December 2001

Abstract

In July 1996 a major rainstorm and flood took place in the Saguenay Fjord. Backscatter strength measurements made with a Simrad EM1000 multibeam echosounder in 1993, 1997 and 1999 have shown spatial and temporal variations, which are interpreted in relation to the occurrence of the flood. After empirical calibration of the different maps the data show an overall diminution of 5 dB in backscatter strength in 1997, 1 yr after the flood took place, while the data sets obtained in 1993 and 1999 show comparable levels of backscatter strength. The different data sets show a similar pattern of low and high backscatter patches, which represent variations of the backscatter strength of a few decibels. Several grain size and water content measurements were also carried out on sediment box core and grab samples from the Fjord bottom in 1997 and 1999. These have shown that the areas with higher acoustic backscatter correspond to the finer sediments, while the low backscatter patches correspond to the coarser material. The data show little relation between water content and backscatter strength, thus indicating a poor dependence between the impedance terms (bulk density and sound speed) and the backscatter. Having taken this into account, the major contribution to backscatter strength is assumed to result from differences in surface and volume roughness of the sediment. Since finer grain sizes offer higher backscatter the grain size of the sediment is not considered as being a major contributor to roughness and hence, backscatter strength. The major factor that seems to control roughness generation in the Saguenay Fjord is considered to be bioturbation. The areas where geological processes most physically disturb the bottom, which coincide with the areas where also most accumulation takes place and the coarser grain sizes are deposited, are more sparsely colonized by organisms. This results in a lower degree of bioturbation, lower roughness and thus, backscatter strength. This hypothesis helps explain the variation in backscatter strength observed between the different measurement years. The several million tons of sediment deposited in the Fjord bottom after the 1996 flood buried the benthic fauna, which was still recovering 1 yr later. The less bioturbated sediment at this time would present lower roughness with respect to the 1993 and 1999 data resulting in a lower backscatter strength.

* Corresponding author. Fax: +34 93 402 1340.
E-mail address: roger@beagle.geo.eb.es (R. Urgeles).

0025-3227/02/$ – see front matter
PII: S0025-3227(01)00303-6

Keywords: multibeam bathymetry; backscatter; grain size; water content; bioturbation; Saguenay Fjord

1. Introduction

Data from multibeam bathymetry and side-scan sonar systems is becoming increasingly used to characterize the sea bottom from a quantitative and qualitative point of view (Hines, 1990; Gardner et al., 1991; Stewart et al., 1994; Mitchell, 1993; Hughes Clarke et al., 1997; Borgeld et al., 1999; Goff et al., 1999, 2000). The causes of backscatter variations on the sea floor can be best investigated in structurally simple areas where variations can be modeled with fewer free parameters (e.g., Mitchell, 1993; Mitchell and Hughes Clarke, 1994; Stewart et al., 1994). These conditions are found where contrasting geologic materials exist. However, in areas where only fine-grained sediments are present, regional differences in acoustic backscatter are often also measured. The difference in overall levels of scattering strength between a muddy seafloor and a rocky seafloor is typically of the order of 20 dB (Urick, 1975), while in uniformly sedimented bottoms the analysis and zonation of the backscatter relies on regional variations of as little as 1 dB (Borgeld et al., 1999; Goff et al., 2000; this study; see also Gardner et al., 1991). Although these differences are limited to a few dB, the processing techniques used to display the imagery data allow one to emphasize and clearly map these minor, but significant, changes in acoustic backscatter. This work is further complicated because the signal recorded over sediments commonly involves scattering both at the surface and in the volume of the sediment (Jackson et al., 1986a,b; Hines, 1990; Gardner et al., 1991; Mitchell, 1993). These can not be easily separated without substantial knowledge of the seafloor's surface roughness, density and other properties (Jackson et al., 1986a) and therefore, ground-truthing using sediment samples appears indispensable.

In multibeam systems the sonar geometry is determined through precise navigation and attitude measurements, while the large-scale bathymetry can be mapped at a level of detail unavailable by any other means. On the other hand, the physical properties of the bottom are not easily assessed and usually require additional techniques to be employed. The sediment type will control the bottom roughness and the water/sediment sound speed and density ratios as well as the attenuation due to the dissipation of acoustic energy through the interface (Stewart et al., 1994).

In this manuscript we present three sets of backscatter data acquired with a Simrad EM1000 in 1993, 1997 and 1999 in the upper Saguenay Fjord, Québec. The data are additionally supported by box cores and grab samples. In between the data sets of 1993 and 1997, a major flood occurred in the study area (July 1996) depositing a fresh sediment layer of up to 16 million m^3 (Côté et al., 1999) along large extensions of the Fjord bottom. This allows us to investigate not only the causes of spatial backscatter variations, but also the causes of temporal backscatter variations in the Fjord. Understanding this is of crucial importance to provide a more comprehensive picture of the spatial extension and effects of the 1996 flood in the Saguenay Fjord.

2. Geological framework

The Saguenay Fjord lies within the Canadian Shield, which is mostly composed in this area by Precambrian rocks of metamorphic origin. The region was tectonically active between 175 and 190 Myr ago, which ended up with the formation of the Saguenay graben structure (Du Berger et al., 1991). During the Pleistocene, ice sheets covered the area several times (LaSalle and Tremblay, 1978). The Saguenay graben, oriented more or less parallel to the glacial flow, became a preferred path for ice flow and resulted in deep excavation of the bedrock. The final retreat of the Wisconsinan ice sheet, which took place about 10 000 yr ago (LaSalle and Tremblay, 1978), was followed by significant isostatic emergence, varying from 140 m on the north side of the graben to 120 m on the south side (Bouchard et

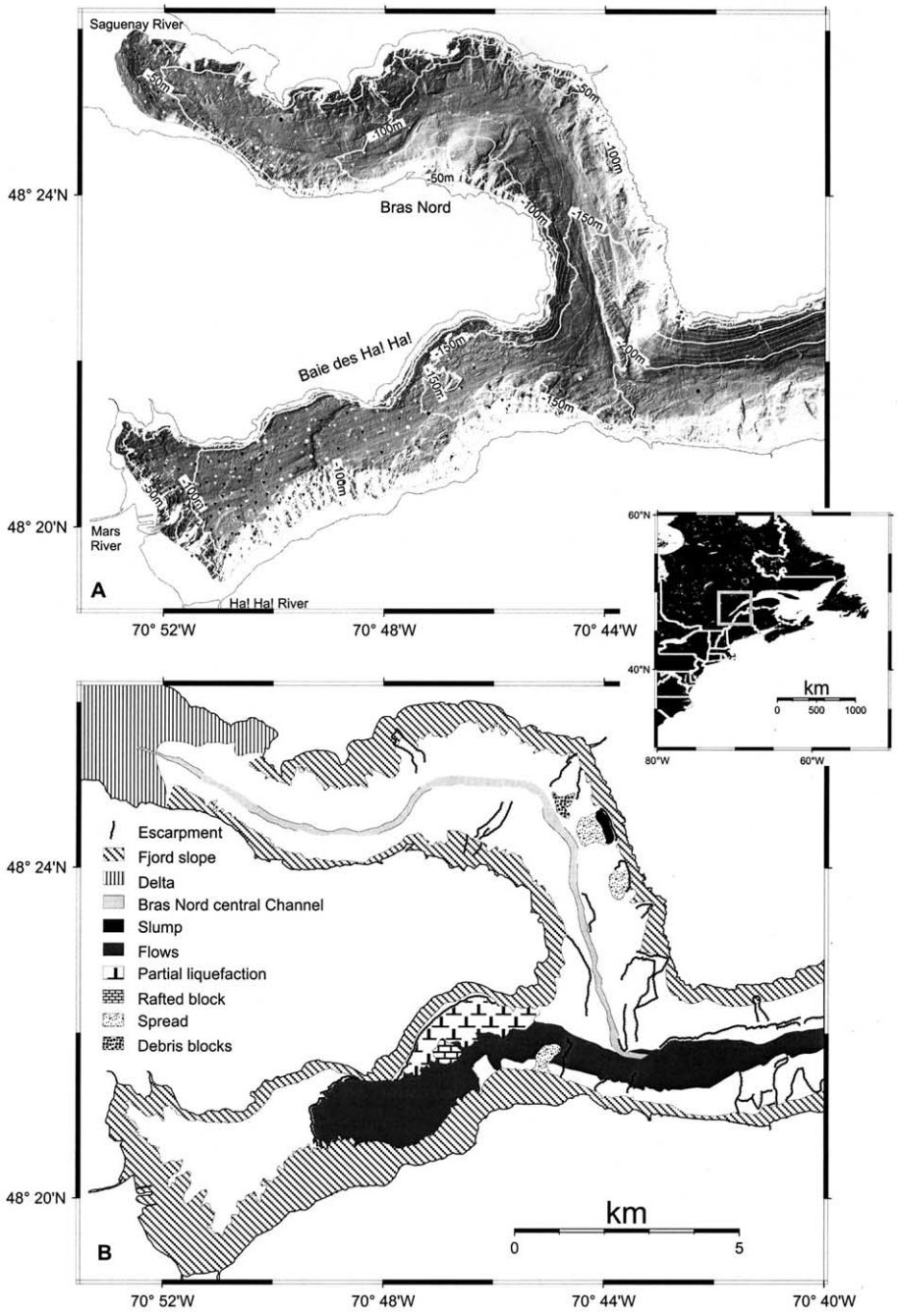

Fig. 1. (A) Bathymetry of the studied area with shaded relief illuminated from the West. Contours are also plotted at 10-m interval. Circles show location of grab samples, inverted triangles show location of box cores. White is for samples collected in 1999 black for those collected in 1997. (B) Geomorphological map of the Saguenay Fjord. Note abundance of escarpments and failure related deposits. Inset shows location of the study area.

al., 1983). This retreat was accompanied by the rapid infill of as much as 1000 m of sediments (Syvitski and Praeg, 1989; Locat and Syvitski, 1991).

Seismic activity has had a profound impact on the morphology of the region in the form of gravitational phenomena both onshore (LaSalle and Chagnon, 1968; Tuttle et al., 1990; Lefebvre et al., 1992; Locat et al., 1997) and on the Fjord bottom (Schaffer and Smith, 1987; Pelletier, 1993; Locat et al., 2000; St-Onge and Hillaire-Marcel, 2001) (Fig. 1b). The latest major sedimentary event in the Saguenay Fjord is associated with the flood of July 1996. The flood deposited a layer of a few decimeters in thickness along the Baie des Ha! Ha! and along large portions of the Bras Nord. At the river mouths, sediment accumulations exceeded several meters (Fig. 2). Prior to the flood, the Fjord bottom sediments were largely contaminated with industrial material (Loring and Bewers, 1978; Barbeau et al., 1981a,b) and it is believed that the huge amount of 'clean' newly deposited sediments has buried the old contaminated ones, thus providing a natural concealing layer.

The morphology of the Upper Saguenay Fjord is characterized by a Y-shape with one arm of the Y being the Bras Nord and the other one being the Baie des Ha! Ha! (Fig. 1A). The Fjord in that area has water depths ranging from 0 to 225 m and a width between 3 to 5 km. The much larger Saguenay River flows into the Bras Nord while the Mars and Ha! Ha! rivers both flow into the Baie des Ha! Ha! The typical tidal range in the area is about 4–5 m. The most active segment of the upper Saguenay Fjord is the Bras Nord where the accumulation rate is measured to be several centimetres per year at the delta (Locat and Leroueil, 1988; Perret et al., 1995) in contrast to the Baie des Ha! Ha! where sedimentation rates are of the order of 0.2 cm/yr (Barbeau et al., 1981a). Thus the Bras Nord is being filled more rapidly that the Baie des Ha! Ha!

The water depth in the Bras Nord ranges from about 10 m at the mouth of the Saguenay River to 200 m at the confluence with the Baie des Ha! Ha! The Baie des Ha! Ha! itself has a water depth which rapidly descends to about 100 m near the head (at La Baie city) to 200 m downstream (Fig. 1B). The sea floor of the Baie des Ha! Ha! has a unique feature located around 70°49′W, 48° 20.5′N, in the form of a sharp and more or less straight escarpment (Fig. 1A). Above it, the slope is 0.6° and below 0.2°. The slopes on either side of the Fjord are quite different, in particular in the Baie des Ha! Ha!, the northern escarpment is steep with slopes exceeding 40° while the south shore slope is gentler and gullied. The slope on the north side is controlled by the bedrock while the southern side is dominated by Quaternary sediments. The Bras Nord is bisected by a shallow channel (Fig. 1) along its axis, potentially acting as a conduit for mudflows or debris flows originating from the upper reaches of the Fjord.

3. The backscatter equation

As multibeam sonars project acoustic energy at different angles on a narrow azimuth range most of the energy that is returned back to the sonar does not come from direct echoes. Since there is always some amount of bottom roughness, this acts to scatter the arriving sound in all directions producing the phenomena that we know as backscatter. The time series of backscattered energy after the first arrival can be therefore used to infer changes in seafloor properties along that azimuth (Hughes Clarke, 2000). This acoustic energy is measured by multibeam systems and recorded as the backscatter strength (BS), which is a calibrated quantity that depends on the topographic and acoustic properties of the seafloor (Urick, 1975; see also Stewart et al., 1994) and defined as:

$$\mathrm{BS} = 20\log\frac{f}{B} - \mathrm{SL} - \mathrm{RCV_{bp}} - \mathrm{XMIT_{bp}} - \mathrm{TVG} + 2\alpha r + 2\mathrm{TL} - 10\log A \quad (1)$$

where f is the received raw echo amplitude, B is a scaling factor to account for A/D conversion, SL

is source level, RCV_{bp} and $XMIT_{bp}$ are receiver and transmitter beam pattern compensations, TVG is the time-varied gain, α is the absorption coefficient for water, r is slant range, TL is transmission loss due to spherical spreading of the acoustic wave and A is the equivalent ensonified area or 'acoustic footprint' of the pulse (Urick, 1975).

From the expressions above three sorts of factors are involved in the equations: (1) factors associated with the transmitter–receiver characteristics (B, SL, RCV_{bp}, $XMIT_{bp}$, r); (2) factors associated with seafloor geometry (A); (3) factors associated with attenuation of sound in water (α, TL).

The sediment properties contributing to backscatter strength (built into the 'f' term) are relatively well known but it is generally complicated to determine what the relative influence of each of the different variables on the resultant backscatter strength is. The matter is further complicated by the fact that both surface and volume components contribute to the total backscatter strength (Jackson et al., 1986a). This problem is usually approached from the scattering cross-section per unit angle per unit area of scattering σ, which is related to the backscatter strength (BS) by:

$$BS = 10\log\sigma \tag{2}$$

Jackson et al. (1986b) calculate the scattering cross-section independently for the surface $\sigma(\theta)$ and the volume $\sigma_{vs}(\theta)$ components and then add them together, i.e., assume that surface roughness does not modify the energy that goes through the interface:

$$\sigma = \sigma(\theta) + \sigma_{vs}(\theta) \tag{3}$$

According to the composite roughness model of Jackson et al. (1986b) there are three major components influencing the scattering cross-section. Impedance terms (mainly bulk density and p wave velocity), surface roughness terms (from grain size to bedforms to bioturbation) and volume hetereogeneities (layering, burrows, mud clasts, ...). For a complete formulation see Jackson et al. (1986b).

4. Methods

The data presented in this paper is largely based on multibeam bathymetry acquired with the Simrad EM1000 in three cruises in July 1993 (before the flood), and August 1997 and August 1999 (after the flood) on board the catamaran CCGS *Frederick G. Creed*. The EM1000 works at a frequency of 95 kHz, and may be operated in water depths between 3 and 1000 m. In shallow mode, it uses 60 beams spaced 2.5°, thus covering a sector up to 150° or ~7.5 times the water depth. The beams are 3.3° and 2.4° width in the across and foreaft direction respectively. The data are positioned using differential GPS. Using advanced processing techniques a vertical resolution of 0.25% the water depth can be achieved for features that span an horizontal distance of about 10% of the water depth, the average beam footprint size (Hughes Clarke et al., 1996).

The EM1000 is also capable of providing a quantitative measure of the sea-floor backscatter strength, which can be displayed in side-scan sonar like images (Hughes Clarke et al., 1996). These images are typically resolved to a higher resolution of about 5% the water depth. The EM1000 corrects the amplitude series for gain changes, propagation losses, predicted beam patterns and for ensonified area (see Eq. 1). Subsequent processing uses real sea floor slopes and applies empirically derived beam-pattern corrections to produce a quantitative estimate of seafloor backscatter strength across the swath. The variation with grazing angle is removed by extracting the average intensity values for angle bins. This contains a composite of both the residual beam pattern effects and the mean seabed angular response, which allows the local angular difference from the mean level to be calculated for each angle, and then subtracted from the side-scan imagery. While this technique is useful to delineate regional sediment boundaries (Hughes Clarke et al., 1997) it is also true that the variation in backscatter strength as a function of grazing angle also provides additional potential for sediment classification (Hughes Clarke et al., 1996), which we are not taking into account. Another problem is that we assume that the shape of

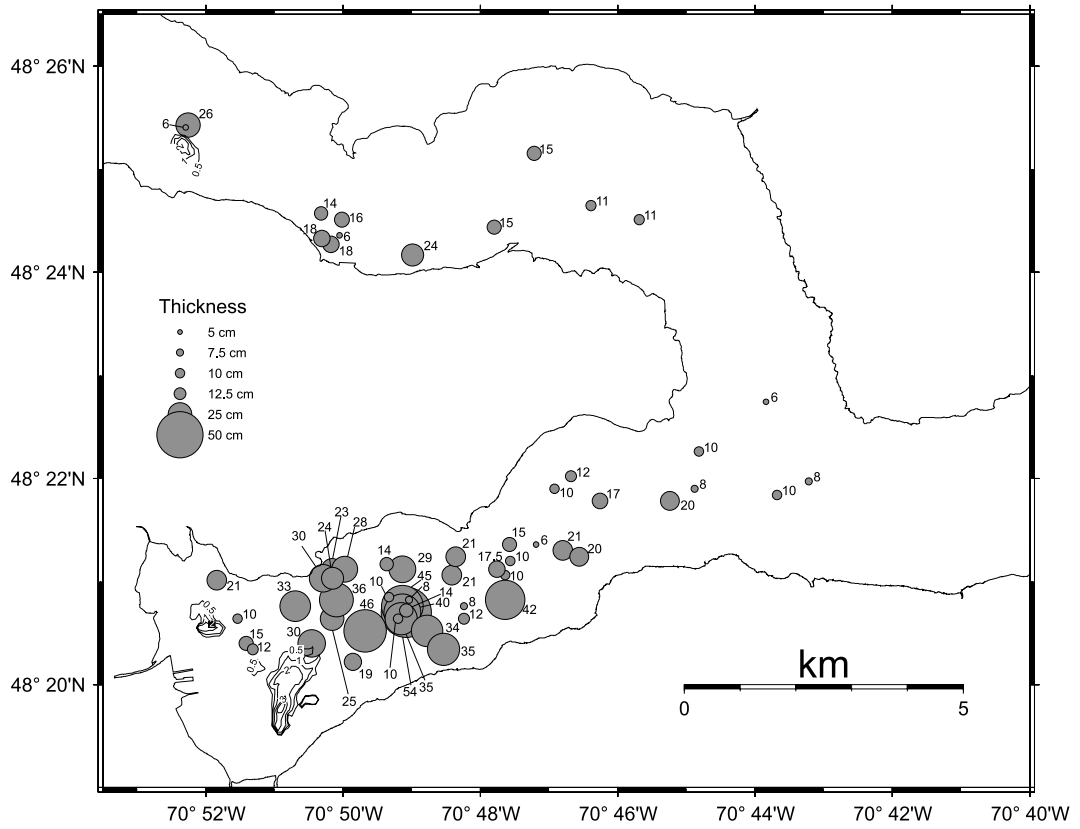

Fig. 2. Extent of the deposits of the 1996 flood. Isocontours are shown for areas where layer thickness is higher than 0.5 m from the comparison of swath bathymetry data acquired in 1993 (previous to the flood) and 1999. For thicknesses lower than 0.5 m the thickness is shown as proportional circles indicating the thickness measured in the box cores.

the angular response curve does not change along the corridor of seabed within which the averaging is done. If this is not the case a residual would remain in the resulting normalized data.

Both the bathymetric and backscatter data were acquired using Simrad's Merlin software and processed using the Ocean Mapping Group of the University of New Brunswick 'Swathed' tools. The data was then imported into GMT (Wessel and Smith, 1991, 1998) to generate bathymetric and backscatter plots.

Comparison between the different backscatter data sets could not be performed straightforwardly because changes in hardware, software and different calibrations were applied to the EM1000 system between the different years. Prior to 1994 an unrecoverable automatic gain control error was applied to all EM1000 backscatter data collected within 25° of vertical incidence (Hammerstad, 1994). This was removed in 1994, and for the period mid 1994–mid 1996 this caused the data acquired in this region to be underpredicted by about 15 dB (Hughes Clarke et al., 1997). In mid 1996 a software change seemed to

Fig. 3. Sequence of backscatter maps for: (A) 1993. (B) 1997. (C) 1999. Note lower backscatter in the proximal areas and enlargement of the extension of the low backscatter acoustic facies in 1997. Box in C shows calibration area. For the three surveys, the backscatter gray-scale palette is histogram equalized with respect to the 1999 survey.

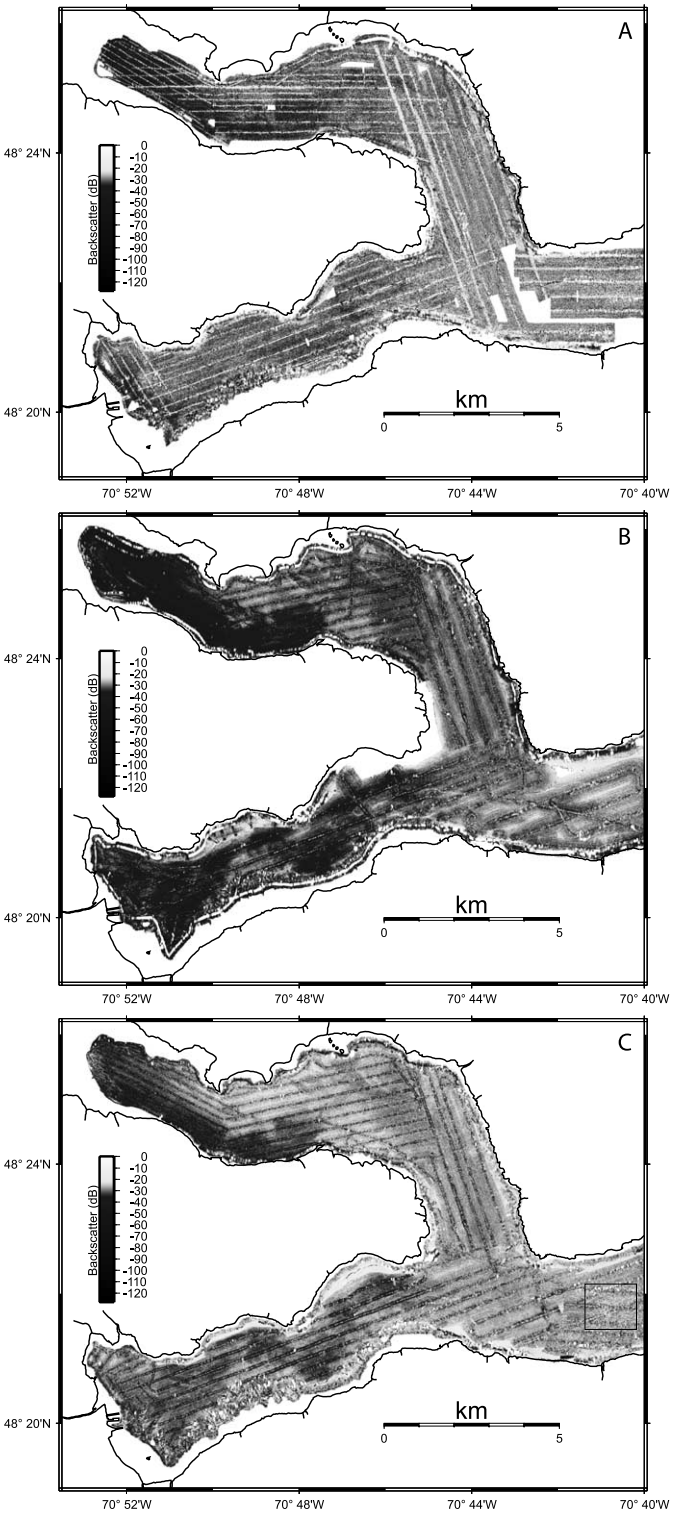
A
B
C
Backscatter (dB)
0
-10
-20
-30
-40
-50
-60
-70
-80
-90
-100
-110
-120
km
0
5
48° 24'N
48° 20'N
70° 52'W
70° 48'W
70° 44'W
70° 40'W

rectify this problem (Hughes Clarke et al., 1997). To overcome these inconveniences and to make comparisons between different data sets, an empirical method for calibrating the data was conceived (Kammerer et al., 1998; Schmitt et al., 2000). Since it was believed that the most distal parts of the Fjord were insignificantly affected by the flood of 1996 (see also Fig. 2), we supposed that the parameters controlling acoustic backscatter there had not changed. Therefore, the mean of the backscatter for this area was assumed to remain constant and thus believed to be equal to the value measured in the last survey. The mean difference between different surveys in this calibration area was removed and made comprehensively to the whole of the survey area in order to suppress the effects induced by those changes.

Water content and grain size were measured in seafloor surface samples obtained from grab and box sampling devices. Grab sediment samples were obtained by means of a Shipek sediment sampler on board the R.V. *Alcide C. Horth* in August and October 1997 and May 1999, on the R.V. *Martha Black* in August 1997, and on board the CCGS *Dennis Riverain* in August 1999. The Shipek can obtain a sample of approximately 0.01 cubic meters. Surface samples from box cores were obtained on board the *Alcide C. Horth* in October 1997, May, June and August 1999. The box corer has typical dimensions of $0.5\times0.5\times0.5$ m, which produces almost no sample remolding. The use of the Shipek grab sampler is justified however, because for the surface spatial analysis much more samples could be collected from a smaller ship. A differential GPS system was used for positioning the vessel at the time of the sampling, but no account was taken for sampler offset from the vessel. Based on our observations of typical wire angles and the known depths, the total sample position uncertainty is estimated to be 15–20 m.

Water content was measured after drying the samples at 105°C for a period of 24 hr. Grain size measurements were made using the hydrometer method. Sediments that showed evidence of high organic matter contents were first treated with hydrogen peroxide. Subsequently all sediments were set in suspension in a solution of hexametaphosphate (5 g/l), which has the effect of reducing the links between clay particles due to the flocculation. The density variation of the solution was measured at different time intervals and, finally, the Stockes' law was used to compute the mean diameter of the sediment particles from their settling speed and the changing density of the solution with time. For comparisons between backscatter and core data, the mean intensity of seabed backscatter was derived from a $\sim100\times100$ m area around each core location.

5. The results

5.1. EM1000 backscatter

The EM1000 backscatter data are shown for the three successive surveys in Fig. 3. The imagery is displayed following a palette equalized according to the cumulative data distribution curve of the 1999 data, so that the different gray levels are adjusted to occupy the same area on this map ('histogram equalization'). This technique enhances the contrast due to small changes in backscatter. The backscatter scale bar also provides an idea of how the data are distributed. Since most of the changes in gray scale are observed around the value of -30 dB (for year 1999) this indicates that most of the values occur around an interval centered on this quantity (see also Table 1).

At a first glance, regional variations of the backscatter are clear in the Saguenay Fjord (Fig. 3). Although these variations appear strong on the backscatter images (Fig. 3) they are only of the order of a few dB. This is due to the histogram equalization. It is to be noted that, for example for the data acquired in 1999, 90% of the data lies within the interval between -39 dB and -24 dB (Table 1).

Both, at La Baie des Ha! Ha! and the Bras Nord, the backscatter increases towards the distal parts away from the river mouths. In the La Baie des Ha! Ha! a more complex pattern than in the Bras Nord is shown. Overall the backscatter increases towards the west, as in the Bras Nord, but the low backscatter area tends to be constrained in the center of the Fjord, describing a sinuous

Table 1
Backscatter statistics

	1999	1997 calibrated	1997	1993 calibrated	1993
Mean	−30.82	−35.23	−30.23	−30.51	−24.94
Std. dev.	4.95	6.28	6.28	5.02	5.02
$I^{a}_{90\%}$	[−39.18, −24.28]	[−46.78, −26.80]	[−41.76, −21.79]	[−38.08, −22.53]	[−32.50, −16.95]
$I^{b}_{50\%}$	[−33.24, −27.96]	[−38.75, −31.05]	[−33.74, −26.04]	[−33.25, −27.80]	[−27.67, −22.23]
Min.	−124.57	−91.13	−86.12	−128	−126.34
Max.	−5.6	−6.77	−1.75	−6.81	−1.24
Calibration area					
Mean	−29.31		−24.29		−23.73
Std. dev.	3.04		4.22		3.60

[a] Interval containing 50% of the backscatter measurements.
[b] Interval containing 90% of the backscatter measurements.

curve more or less parallel to the Fjord margins (Fig. 3). Where the southern shore describes a convex northwards promontory or the reverse outline in the northern shore, high backscatter, apron-like areas tend to develop displacing the low-backscatter areas northwards or southwards respectively (Fig. 3). This pattern is further complicated by the fact that the southern side of the Fjord has a complex gullied morphology (Fig. 1B) with variable backscatter intensity (Fig. 3).

In the case of the Bras Nord, the backscatter contrast is more prominent than in the Baie des Ha! Ha! (Fig. 3). It is especially low immediately west of the Saguenay River delta and all along the southern half of the upper Bras Nord, probably reflecting the pathways of sediment delivered from the river to the Fjord. The low backscatter facies are surrounded by the high backscatter facies, which merge distally with the high backscatter facies at the Baie des Ha! Ha! Bathymetry and geomorphological evidence (Fig. 1) suggest a complex sediment deposition pattern in the Baie des Ha! Ha!, while in the Bras Nord this is controlled by the larger point-source sediment input of the Saguenay River, which creates a more uniform sediment-type gradient from proximal to distal parts. As a result, the backscatter maps (Fig. 3) show relatively less contrast in backscatter strength between the low and high-backscatter areas in the Baie des Ha! Ha! than in the Bras Nord (Fig. 3) as well as a more complex distribution of the two acoustic facies.

The regional backscatter zonation observed in the EM1000 data is persistent through 1993, 1997 and 1999 with slight differences. The relative boundaries between the different acoustic backscatter regions and the overall backscatter strength appear to change slightly (see Table 1 and Fig. 3). In 1993 (Fig. 3A) the boundaries between the different acoustic regions are more

Table 2
Sediment sample statistics

	Year	Mean (%)	Max (%)	Min (%)	Std. dev.	No. samples
Water content	1997	75.36	206.52	16.80	27.91	74
	1999	96.32	204.78	26.75	37.31	234
Clay content	1997	20.26	68.86	9.13	8.43	46
	1999	26.18	40.56	4.36	7.94	187
Silt content	1997	70.46	24.87	86.69	17.38	46
	1999	71.24	95.64	30.34	9.44	187
Sand content	1997	9.26	57.69	0.03	14.03	46
	1999	2.58	57.70	0	8.21	187

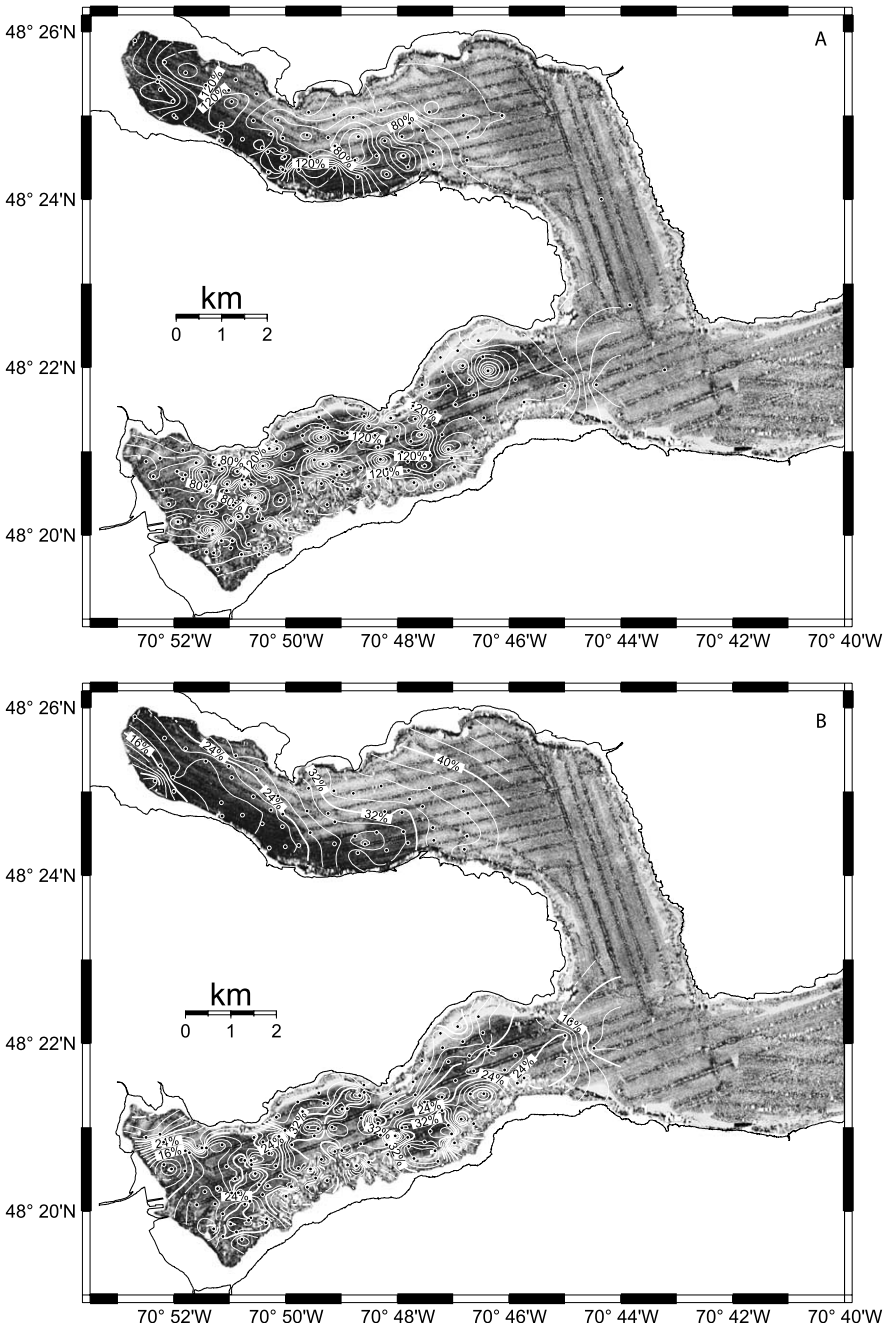

Fig. 4. (A) Backscatter map for 1999 with superimposed isocontours of water content (% ratio of total weight to dry weight) as measured in 1999. (B) Backscatter map for 1999 with superimposed isocontours of grain size (% clay) as measured in 1999. Isocontours maps were created using the continuous curvature splines of Smith and Wessel (1990).

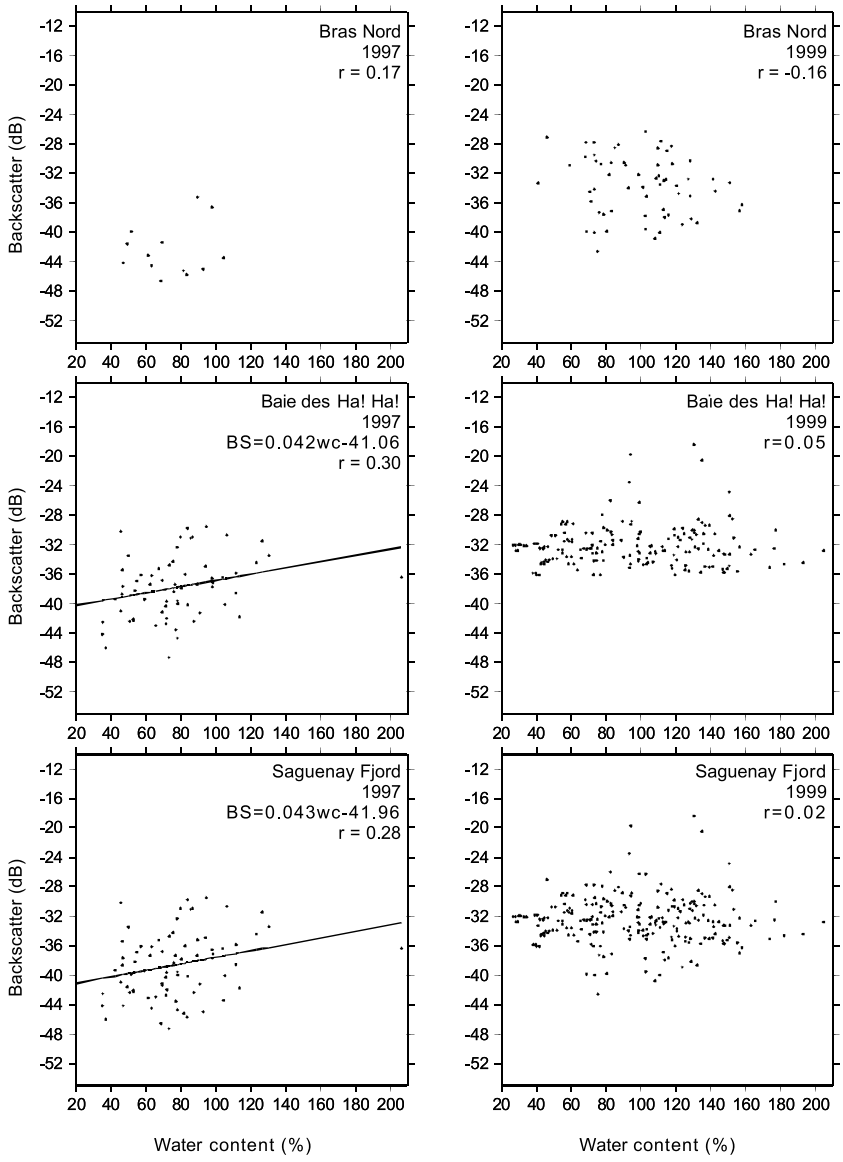

Fig. 5. Correlation by least mean square regression between water content as measured for the Bras Nord (top), the Baie des Ha! Ha! (middle), and the whole Saguenay Fjord (bottom), for years 1997 (left) and 1999 (right). Regression line for scatterplots with $r < 0.2$ is not shown.

diffuse than in the two following years. In August 1997 (Fig. 3B), just 13 months after the flood of 1996, the proximal low-backscatter facies show a larger extension and an overall lower backscatter within the whole region. In contrast, in 1999 (Fig. 3C) the boundaries between the different acoustic regions seem to evolve backwards to come close to those of 1993, and in overall the backscatter is similar, although slightly lower, than the average backscatter measured in 1993.

5.2. Sediment samples vs. EM1000 backscatter

It is to be noted here that, since the backscatter strength integrates over some sediment volume, for the purpose of cross correlation with sediment

properties it is assumed that there are no significant variations in grain size or water content as a function of depth within the sediment (i.e., there are no layer interfaces at the maximum depth of signal penetration). Since bioturbation tends to mix the upper sediment column, thereby homogenizing the sediment, this is presumed to be a valid assumption. Therefore, we have assumed that the volume over which the EM1000 backscatter integrates contains no layering and that the sediment grain size and water content measured are characteristic of the interval over which the backscatter strength is obtained. Variations in water content due to the overburden are considered to be proportional, hence the relative spatial variations hold with depth, and therefore cross correlation with backscatter strength is not affected.

5.2.1. Water content

Water content was measured in 234 samples from the Saguenay Fjord in 1999 and in 74 samples in 1997. The values range from as little as 17% to as much as 207% for 1999, while similar values for 1997 (27–205%) were observed (Table 2). However, the mean water content appears significantly lower for 1997 than for 1999 (Table 2), indicating that sediment loosening may have occurred at the sediment–water interface. Both years show the lack of any significant trend in water content from west to east, from proximal to distal areas (Fig. 4A), and several localized anomalies are observed (Fig. 4A).

Water content is a property of the sediment that is directly related to the porosity and sediment bulk-density. In the light of the discussion above, one would therefore expect to find some degree of correlation between water content and backscatter. The data obtained in 1999 does not show a clear correlation and scatterplots mostly display a cloud of points (Fig. 5). For 1997, however there seems to be a slightly positive trend in

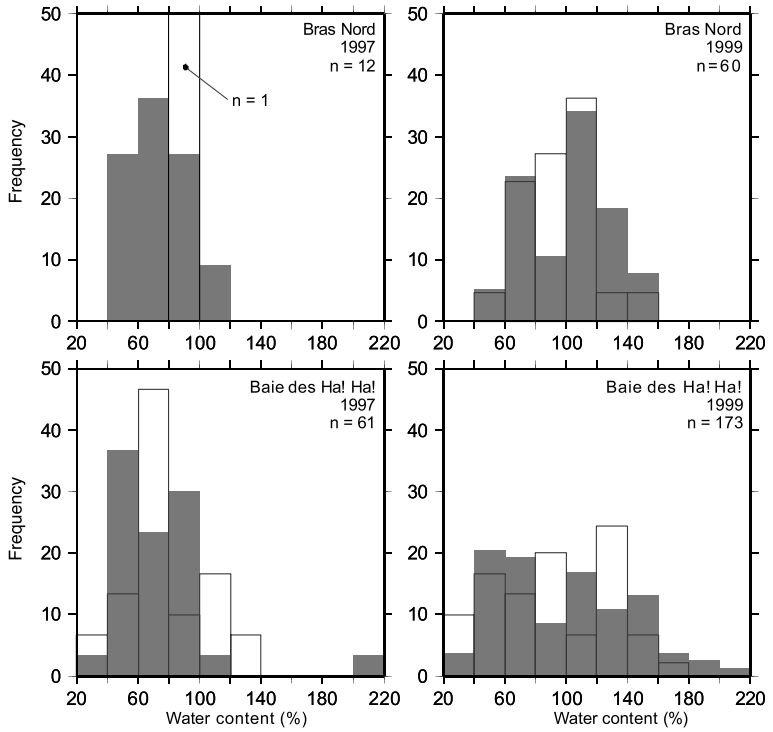

Fig. 6. Frequency histogram of water content as measured in grab samples for the Bras Nord (top) and the Baie des Ha! Ha! (bottom) for 1997 (left, total 74 samples) and 1999 (right, total 234 samples). High backscatter areas are shown as filled bars, low backscatter areas are shown as transparent bars.

the Baie des Ha! Ha! (not enough samples were collected in the Bras Nord) showing an increase in backscatter strength with increasing water content. Nevertheless, the correlation coefficients are still too low.

This lack of correlation is also clear in Fig. 6. Neither the sediments sampled on the Bras Nord (Fig. 6) nor the sediments sampled in the Baie des Ha! Ha! in 1999 (Fig. 6) show markedly different water content distributions in the high and low backscatter areas, only those of the Baie des Ha! Ha! show slightly higher water contents within the areas of high backscatter.

5.2.2. Grain size

The analyses of the sediment samples (Table 2)

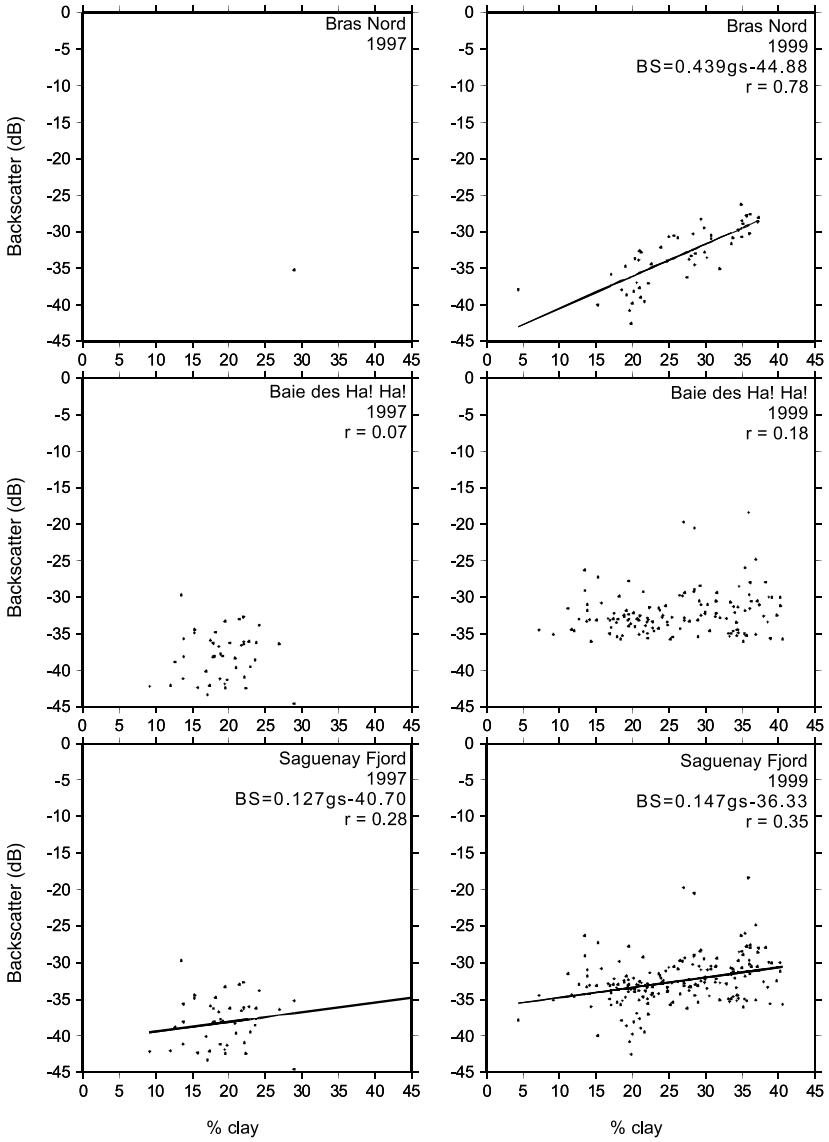

Fig. 7. Correlation by least mean square regression between grain size as measured for the Bras Nord (top), the Baie des Ha! Ha! (middle), and the whole Saguenay Fjord (bottom), for years 1997 (left) and 1999 (right). Regression line for scatterplots with $r < 0.2$ is not shown.

collected in the Baie des Ha! Ha! and the Bras Nord show almost no differences in grain size between 1999 and 1997. The predominant sediment fraction in the Fjord is silt, both in 1997 and 1999 (total average 71.2% in 1999 and 70.46% in 1997) and then clay (total average 26.2% in 1999 and 20.3% in 1997), while only very little amounts of sand are present at the river mouths (total average 2.6% in 1999 and 9.3% in 1997). As there are only two significant grain size classes, for all further comparisons between backscatter and grain size we use the clay content, although the plots against silt content would yield a very similar trend. In doing so, we also compare backscatter against cohesion, which is determined by the amount of clay minerals.

From a rapid glimpse at the different EM1000 surveys (Fig. 3) a negative correlation between observed backscatter strength and grain size (Fig. 4A) is expected. In Fig. 4A it is particularly striking how the contours describing clay content outline the acoustic pattern distribution observed in the backscatter strength map. The river mouths where most coarse material (low clay contents) accumulates, show the lowest backscatter, while the higher clay contents are associated to the higher backscatter.

A regression of the backscatter strength versus clay content (Fig. 7) shows that the sediments containing a higher proportion of the finer fraction are those with higher backscatter. In particular the good correlation obtained for the Bras Nord in 1999 is striking (unfortunately only one sample could be collected in 1997), with a correlation coefficient near 0.8, while little relation appears to exist between both parameters in the Baie des Ha! Ha! neither in 1999 nor in 1997 (Fig. 7). This is in general contradiction with previous studies which have shown an overall increase in backscatter strength with grain size (Stanic et al., 1989; Jackson et al., 1986b; Jackson and Briggs, 1992; Hughes Clarke et al., 1997; Knebel et al., 1999; Goff et al., 2000). This trend is also clear in Fig. 8, which shows lower clay contents where backscatter is low and higher clay contents where backscatter is high. In the Baie des Ha! Ha! the relation between backscatter and grain size is notably less obvious, but a similar trend appears to exist (Fig. 8). The less contrasted backscatter strength and more complex pattern distribution of low and high backscatter acoustic facies (Fig. 3) may help explain the lack of a better correlation in the Baie des Ha! Ha!

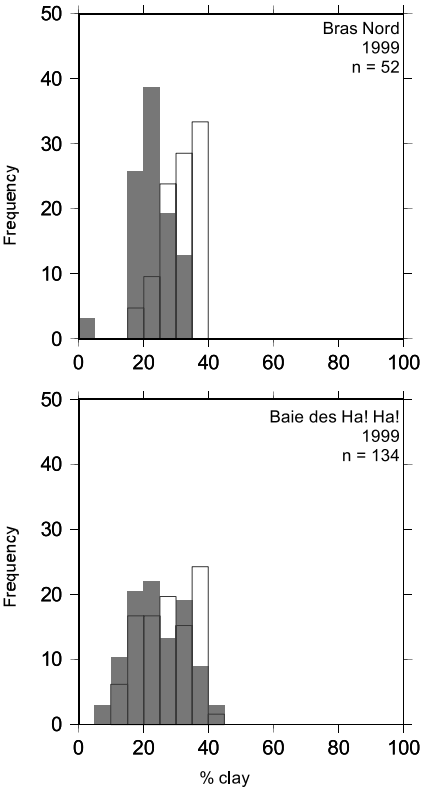

Fig. 8. Frequency histogram of grain size as measured in grab samples for the Bras Nord (top) and the Baie des Ha! Ha! (bottom) in 1999. High backscatter areas are shown as filled bars, low backscatter areas are shown as transparent bars (total 186 samples).

6. Discussion

6.1. Inferred causes of the spatial backscatter variations

As already mentioned, several factors probably contribute to backscatter strength in proportions that depend on the sedimentary setting being considered (see 1. Introduction). These include roughness and the sediment–water speed and density

ratios. A complete model should also consider scattering from within the volume of the sediment (Jackson et al., 1986b). In this section we are not only considering those physical constraints that condition the backscatter strength but also the biogeological processes that affect these physical properties. The factors that should be considered in the context of the Saguenay Fjord are explained here below in apparent order of decreasing importance.

6.1.1. Bottom roughness

The main parameter that correlates with backscatter strength is grain size ((Fig. 4B in the Bras Nord, Figs. 7 and 8). This is also one of the most reported correlations in the literature (Jackson et al., 1986b; Jackson and Briggs, 1992; Hughes Clarke et al., 1997; Knebel et al., 1999). The backscatter responds to grain size because the later induces different amounts of roughness to the sea bottom, with the larger roughness being associated to the coarser sediments.

The case of the Saguenay Fjord is analogous to the Eel River shelf (Borgeld et al., 1999) where the finer materials of a flood deposit are associated with the highest backscatter. Therefore, it would seem that lower roughness values would yield higher backscatter producing results that are apparently in contradiction with presently available models (see Jackson et al., 1986b). However, Jackson et al. (1986b) state that for bottoms having relatively fine sediments, there is a surprisingly weak dependence of scattering strength on sediment type, with an increase of only 3–6 dB when moving from clay and silt to sandy bottoms. Within each sediment class, however, particular sites may differ by as much as 10–15 dB, strongly suggesting that sediment type, as determined from grain size distribution, is not a sufficient descriptor as far as backscatter strength is concerned (Jackson et al., 1986b). The fact is, however, that the data does shows a certain correlation (Figs. 4B and 7) thus it appears that probably different processes take place in different sediment types, whose effects on the backscatter strength would prevail over those of the roughness associated with grain size.

At the wavelength being considered for the EM1000 (1.6 mm) the most important inhomogeneity is not the graininess of the sediment, but larger-scale inhomogeneities (Jackson et al., 1986b) such as those caused by burrowing, shells and ripple marks. Two major feature types may contribute roughness to the Fjord bottom. These are the sedimentary structures such as ripple marks and bioturbation structures. The firsts tend to occur often on non-cohesive materials and are subject to available physical energy of the media, while the second would, a priori, mostly occur in areas where physical disturbance is minor.

Influence of sedimentary structures in bottom roughness and backscatter strength has been described by Borgeld et al. (1999) in the Eel Shelf, off California. According to these authors, the rapid deposition of a muddy layer associated with a flood resulted in better preservation of incorporated ripple forms than in areas less directly impacted by the flood deposit. Both the Saguenay Fjord and the Eel Margin have in common that the finer sediments are those yielding the higher acoustic backscatter. However, the situation in the Saguenay Fjord differs from that of the Eel margin in that the area of sediment deposition associated with the flood corresponds for the most part to the area of lower backscatter (Figs. 2 and 3). If sediment structures were to exist on the coarser sediments, this would induce an increase in bottom roughness, and thus in backscatter strength. Therefore, roughness associated with flow structures can not be considered to explain the 'inverse' correlation between grain size and acoustic backscatter.

On the other hand, organisms tend to prefer quiet areas with little physical disturbance (see for example Aller and Aller, 1986; Alongi and Robertson, 1995; Gerino et al., 1999), which, in the Saguenay Fjord, occur in the most distal high-backscatter areas, away from the river mouths (the most important Saguenay river in the Bras Nord and the smaller Mars and Ha! Ha! rivers in the Baie des Ha! Ha!), where higher energy and episodic sedimentation induce coarser sediment and higher sedimentation rates (Fig. 2, see also Locat and Leroueil, 1988). Organisms may produce pits and depressions related to burrowing

and foraging activity. The benthos also produces elevations such as mounds from burrow excavation, tracking and feeding (Frey, 1975). Typical length scales of these features range from meters down to submillimeter scales (McCall and Tevesz, 1982). The backscatter strength responds to bottom roughness and subbottom heterogeneity at scales on the order of 0.5–2 times the acoustic wavelength at typical grazing angles for side-scan surveys (Jackson et al., 1986a), i.e., at horizontal spans of 0.8–3.2 mm for the EM1000, which is probably within the diameter and height range of bioturbation structures in the Fjord bottom.

It is thus our opinion, that the higher backscatter of the finest sediments is due to bioturbation induced roughness, while on the lower backscatter patches, close to the river mouths and along the sediment pathways, physical disturbance of the benthos prevents a more important colonization, thus a lower degree of bioturbation and roughness generation, and consequently lower backscatter strength. This hypothesis is supported by the association of the flood occurrence with, (1) the variation in overall levels of backscatter strength observed previous and after the flood of 1996 (Table 1), and (2) the drastic decrease in the number of specimens and species associated with the deposition of the flood layer (Pelletier et al., 1999) (see 6.2. Inferred causes of the temporal backscatter variations). If this hypothesis holds true, this would imply that significant changes in the benthic ecosystem could be monitored from backscatter strength measurements.

6.1.2. Subsurface features-volume scattering

In addition to what has been stated in the previous section, buried structures such as burrows, buried ripples and fluid escape structures, may also cause acoustic scattering (volume scattering) when there is significant penetration of the sonar signal into the sediment. It has been shown that, generally, where sediments are fine volume scattering is predominant over surface scattering (Jackson and Briggs, 1992), while for sand bottoms, roughness surface scattering is relatively more important (Jackson et al., 1986b). This suggests that in the mostly clayey silts of the Saguenay Fjord volume scattering due to the bioturbation might be even more important than surface scattering. Mitchell (1993) suggests that for a frequency of 100 kHz at 30° grazing angle, approximately the frequency of the EM1000, the signal loss is 20–30 dB/m in fine sediments. Mitchell (1993) also shows that acoustic energy from the EM1000 can penetrate a maximum of 50 cm in muddy sediments, which would imply an acoustic response contributed by the entire sediment column recovered from our box cores.

6.1.3. Water–sediment sound speed and density ratios

The remobilization induced by bioturbation may cause loosening or hardening of the sediment. Here there is contradictory data in the Saguenay Fjord. While some authors report loosening of the uppermost sediment causing a marked reduction of the ratios of mass density (Montety et al., 2000), and therefore a reduction in compressional wave speed ratios at the water–sediment interface (Richardson et al., 1983), others consider that bioturbation is the most plausible cause for the apparent surficial sediment overconsolidation typically observed on most cores (Perret et al., 1995; see also Baraza et al., 1990; Lee et al., 1999). Nevertheless, bioturbation is associated with an upper mixed layer with high water contents (Ekdale et al., 1984) which most likely will reduce both ratios.

The consolidation state may have an important effect on the sediment strength and generally comports a densification of the sediment. Sediment overconsolidation typically results, for example, from sediment erosion (Lee and Edwards, 1986). Cases where areas of high backscatter were believed to correspond to the presence of overconsolidated sediments have already been reported in the literature (see Lee et al., 1999). Essen (1994) discusses the effects of layering and consolidation in backscatter strength to show that although shear-waves velocities are small in unconsolidated sediments as compared to compressional waves velocity, they are of some influence on the seafloor reflectivity. Regions where this might occur in the Saguenay Fjord include those that have suffered sediment landslides resulting in the re-

moval of the upper sediment layer. However the areas that have undergone these processes, such as the area to the east of the central escarpment in the Baie des Ha! Ha! (Fig. 1A) do not show evidence of an increase in backscatter strength. It must also be noted, however, that since the event took place, probably in 1667 (see discussion in Locat et al., 2000), a continuous input of sediment has taken place and the backscatter may no longer respond to these non-active now-buried features.

All these processes should be accounted for in measuring the water content. Water content is, a priori, an important factor influencing the backscatter strength because it is directly related to the sediment bulk-density and porosity and thus it conditions the water–sediment density and sound-speed ratios, as well as the penetration angle of the refracted incident wave. However the data presented in Figs. 4A, 5 and 6 suggest almost no correlation between water content, and thus density, and backscatter strength. This is in contrast to the highly variable water content measured in samples for both 1997 and 1999 (see Table 2), thus inducing highly variable sediment densities. This is partially explained by the low differences in backscatter strength being considered over the whole study area and, as mentioned earlier, the fact that regions such as the Baie des Ha! Ha! present a complex pattern of low and high backscatter patches.

6.2. Inferred causes of the temporal backscatter variations

The acoustic response of the Fjord bottom measured in the course of the three EM1000 cruises shows an overall decrease of the backscatter strength in 1997 with respect to that measured in 1993 and 1999 (Table 1). The data recorded in 1997 shows a considerable extension of the low backscatter facies (Fig. 3). This implies that sometime between 1993 and 1997 an alteration of the bottom characteristics occurred. However, the evidence that a similar acoustic zonation is present in 1993 and 1999 support the idea that the process controlling the nature of the bottom, and therefore the different acoustic zones, operates permanently. As shown by the grain size-backscatter relation, these processes are related to the sediment transport and distribution on the Fjord bottom, and the only major event in between 1993 and 1999, which significantly disturbed the sedimentation pattern was the flood of July 1996. As a consequence we believe that the observed acoustic variations are related to the flood.

The flood represented the arrival of several tons of sediment to the Fjord bottom, which resulted in burial of large extensions of the Fjord by a newly deposited layer. Such a layer thus produced a high mortality of the benthos (Pelletier et al., 1999) burying as well all traces of bioturbation. This probably resulted in a decrease in the bottom roughness and thus of the backscatter strength because, although there was an input of coarser material to the Fjord bottom, the roughness associated with the graininess of the newly deposited materials was probably much lower than the roughness associated with the bioturbation structures that were now buried. This interpretation is in agreement with studies of the Fjord benthos showing a drastic reduction in the number of species and specimens at several stations when comparing data previous and shortly after the flood took place (Pelletier et al., 1999). Data subsequently collected has shown that benthic organisms and remobilization of the Fjord bottom have returned to the Fjord (Montety et al., 2000), thus, probably increasing bottom roughness again and explaining the increase in overall backscatter level observed between 1997 and 1999 (Table 1). In support of this hypothesis there is also an overall increase in water content from 1997 to 1999, which seems to point to the recolonization of the substratum and the formation of an upper mixed layer (Berger et al., 1979; Ekdale et al., 1984).

7. Conclusions

(1) The present backscatter strength of the Saguenay Fjord as measured from the EM1000 is around −31 dB. Several zones can be delimited according to their backscatter strength, which rely

on acoustic differences of 2 to 3 dB. The zones presenting the lower backscatter are located at the river mouths and more proximal areas, while the high backscatter areas appear in more distal settings.

(2) The overall backscatter strength of the Fjord bottom has not remained constant over time; an overall decrease seems associated with a large flood event and major sediment input to the Fjord, which occurred in 1996. An overall decrease in backscatter strength of 5 dB is found when comparing the 1993 and 1997 data, while present overall backscatter strength is similar to that of 1993.

(3) In the Saguenay Fjord, considering the small differences in backscatter strength measured between zones of low and high backscatter, there appears to be little relation between water content and, thus, density and backscatter strength.

(4) From the studied samples, the sediments with lower clay contents are those which present the lowest backscatter strength, in contrast to the usual observed increase in backscatter strength with increasing grain size.

(5) The major factor, which appears responsible for the present distribution of low and high backscatter patches, is hypothesized to be the interaction between sedimentary input and sediment reworking by organisms. This hypothesis considers that, in the Saguenay Fjord, the roughness induced by bioturbation is higher than the roughness associated with the graininess of the sediment. The hypothesis is also supported by published data, which show a profound effect of the 1996 flood event on the Fjord benthos.

(6) The observed temporal variations in backscatter strength are believed to reflect the variations in roughness associated to bioturbation, thus, the impacts of the flood on the benthos (1997 data) and its subsequent recovery (1999 data).

Acknowledgements

The authors would like to thank the Natural Sciences and Engineering Research Council and Alcan of Canada Ltd. for their support to the strategic project ''Saguenay post-déluge'' (STP-201981). We also acknowledge the financial support of the Québec Ministry of Education, especially for the postdoctoral fellowship provided to R.U. We also thank the captains and crew members of the various vessels with which data for this study was acquired. Critical reviews by N. Mitchell and R. Wheatcroft greatly improved the original manuscript.

References

Aller, J.Y., Aller, R.C., 1986. General characteristics of benthic faunas on the Amazon inner continental shelf with comparison to the shelf off the Changjiang River, East China Sea. Cont. Shelf Res. 6, 291–310.

Alongi, D.M., Robertson, A.I., 1995. Factors regulating benthic food chains in tropical river deltas and adjacent shelf areas. Geo-Mar. Lett. 15, 145–152.

Baraza, J., Lee, H.J., Kayen, R.E., Hampton, M.A., 1990. Geotechnical characteristics and slope stability on the Ebro margin, western Mediterranean. Mar. Geol. 95, 379–393.

Barbeau, C., Bougie, R., Côté, J.-E., 1981a. Varations spatiales et temporelles du céssium-137 et du carbone dans des sédiments du Fjord du Saguenay. Can. J. Earth Sci. 18, 1004–1011.

Berger, W.H., Ekdale, A.A., Bryant, P.P., 1979. Selective preservation of burrows in deep-sea carbonates. Mar. Geol. 32, 205–230.

Barbeau, C., Bougie, R., Côté, J.-E., 1981b. Temporal and spatial variations of mercury, lead, zinc, and copper in sediments of the Saguenay Fjord. Can. J. Earth Sci. 18, 1065–1074.

Borgeld, J.C., Hughes Clarke, J.E., Goff, J.A., Mayer, L.A., Curtis, J.A., 1999. Acoustic backscatter of the 1995 flood deposit on the Eel shelf. Mar. Geol. 154, 197–210.

Bouchard, R., Dion, D.J., Tavenas, F., 1983. Origine de la préconsolidation des argiles du Saguenay, Québec. Can. Geotech. J. 20, 315–328.

Côté, P., Maurice, F., Locat, J., Kammerer, E., Hill, P.R., Simpkin, P., Long, B., Leroueil, S., 1999. Intégration des méthodes géophysiques et géotechniques pour le calcul du volume de la couche de 1996 dans la Baie des Ha! Ha! (données préliminaires). Canadian Meteorological and Oceanographic Society 33rd Annual Meeting Program and Abstracts, 138.

Du Berger, R., Roy, D.W., Lamontagne, M., Woussen, G., North, R.G., Wetmiller, R.J., 1991. The Saguenay (Quebec) earthquake of November 25,1988: seismologic data and geologic setting. Tectonophysics 186, 59–74.

Ekdale, A.A., Muller, L.N., Novak, M.T., 1984. Quantitative ichnology of modern pelagic deposits in the abyssal Atlantic. Palaeogeogr. Palaeoclimatol. Palaeoecol. 45, 189–223.

Essen, H.-H., 1994. Scattering from a rough sedimental seafloor containing shear and layering. J. Acoust. Soc. Am. 95, 1299–1310.

Frey, R.W., 1975. The Study of Trace Fossils. Springer-Verlag, Berlin, Heidelberg, New York, 562 pp.

Gerino, M., Stora, G., Weber, O., 1999. Evidence of bioturbation in the Cap-Ferret Canyon in the deep northeastern Atlantic. Deep-Sea Res. II 46, 2289–2307.

Gardner, J.V., Field, M.E., Lee, H., Edwards, B.E., Masson, D.G., Kenyon, N., Kidd, R.B., 1991. Ground-truthing 6.5 kHz side scan sonographs: What are we really imaging? J. Geophys. Res. 96, 5955–5974.

Goff, J.A., Olson, H.C., Duncan, C.S., 2000. Correlation of side-scan backscatter intensity with grain-size distribution of shelf sediments, New Jersey margin. Geo-Mar. Lett. 20, 43–49.

Goff, J.A., Orange, D.L., Mayer, L.A., Hughes Clarke, J.E., 1999. Detailed investigation of continental shelf morphology using a high-resolution swath sonar survey: the Eel margin, northern California. Mar. Geol. 154, 255–269.

Hammerstad, E., 1994. Backscattering and sonar image reflectivity. EM12/950/1000 Technical Note, 10 pp.

Hines, P.C., 1990. Theoretical model of acoustic backscatter from a smooth seabed. J. Acoust. Soc. Am. 88, 324–334.

Hughes Clarke, J.E., 2000. Present-day methods of depth measurement. In: Cook, P.J., Carleton, C.M. (Eds.), Continental Shelf Limits, The Scientific and Legal Interface. Oxford University Press, New York, USA, pp. 139–159.

Hughes Clarke, J.E., Danforth, B.W., Valentine, P., 1997. Areal seabed classification using backscatter angular response at 95 kHz. In: Pace, N.G., Pouliquen, E., Bergem, O., Lyons, A.P. (Eds.), High Frequency Acoustics in Shallow Water, NATO SACLANTCEN, conference proceedings series CP-45, pp. 243–250.

Hughes Clarke, J.E., Mayer, L.A., Wells, D.A., 1996. Shallow water imaging multibeam sonars: a new tool for investigating seafloor processes in the coastal zone and on the continental shelf. Mar. Geophys. Res. 18, 607–629.

Jackson, D.R., Baird, A.M., Crisp, J.J., Thompson, P.A.G., 1986a. High-frequency bottom backscatter measurments in shallow water. J. Acoust. Soc. Am. 80, 1188–1199.

Jackson, D.R., Winebrenner, D.P., Ishimaru, A., 1986b. Application of the composite roughness model to high-frequency bottom backscattering. J. Acoust. Soc. Am. 79, 1410–1422.

Jackson, D.R., Briggs, K.B., 1992. High-frequency bottom backscattering: Roughness versus sediment volume scattering. J. Acoust. Soc. Am. 92, 962–977.

Kammerer, E., Hughes Clarke, J.E., Locat, J., Doucet, N., Godin, A., 1998. Monitoring temporal changes in seabed morphology and composition using multibeam sonars: a case study of the 1996 Saguenay River floods. Proceedings of the Canadian Hydrographic Conference 1998, Victoria, Canada, 450–461.

Knebel, H.J., Signell, R.P., Rendigs, R.R., Poppe, L.J., List, J.H., 1999. Seafloor environments in the Long Island Sound estuarine system. Mar. Geol. 155, 277–318.

LaSalle, P., Chagnon, J.-Y., 1968. An ancient landslide along the Saguenay River, Quebec. Can. J. Earth Sci. 5, 548–549.

LaSalle, P., Tremblay, G., 1978. Dépôts meubles Saguenay Lac Saint-Jean. Rapport géologique 191, Ministère des Ricesses naturelles du Québec, Québec, Canada, 61 pp.

Lee, H.J., Edwards, B.D., 1986. Regional method to assess offshore slope stability. J. Geotech. Eng. 112, 489–509.

Lee, H.J., Locat, J., Dartnell, P., Israel, K., Wong, F., 1999. Regional variability of slope stability: application to the Eel margin, California. Mar. Geol. 154, 305–321.

Lefebvre, G., Lebouef, D., Hornych, P., Tanguay, L., 1992. Slope failures associated with the 1988 Saguenay earthquake, Quebec, Canada. Can. Geotech. J. 29, 117–130.

Locat, J., Dubé, S., Couture, R., 1997. Analyse de l'écrouement rocheux du Mont Éboulé, Québec. Proceedings of the 50th Canadian Geotechnical Conference, Ottawa, Canada, pp. 118–126.

Locat, J., Syvitski, J.P., 1991. Le Fjord du Saguenay et le golfe du St-Laurent: Étalons pour l'évaluation des changements globaux au Québec. In: Bouchard, M.A., Bérard, J., Delisle, C.E. (Eds.), Collection Environnement et Géologie, v. 12. Asssocition professionelle des géologues et des géophysiciens du Québec, Québec, Canada, pp. 309–318.

Locat, J., Urgeles, R., Schmitt, T., Houareau, L., Martin, F., Hill, P., Long, B., Simpkin, P., Kammerer, E., Sanfaçon, R., 2000. The morphological signature of natural disasters in the Upper Saguenay Fjord area, Québec, Canada. Proceedings of the 53rd Canadian Geotechnical Conference, Montreal, Québec, pp. 109–116.

Locat, L., Leroueil, S., 1988. Physicochemical and geotechnical characteristics of recent Saguenay Fjord sediments. Can. Geotech. J. 25, 382–388.

Loring, D.H., Bewers, J.M., 1978. Geochemical mass balance of mercury in Canadian Fjord. J. Chem. Geol. 22, 309–330.

McCall, P.L., Tevesz, M.J.S., 1982. Animal–Sediment Relations: the biogenic alteration of sediments. Plenum Press, New York, London, 336 pp.

Mitchell, N.C., 1993. A model for attenuation of backscatter due to sediment accumulations and its application to determine sediment thicknesses with GLORIA sidescan sonar. J. Geophys. Res. 98, 22477–22493.

Mitchell, N.C., Hughes Clarke, J.E., 1994. Classification of seafloor geology using multibeam sonar data from the Scotian Shelf. Mar. Geol. 121, 143–160.

Montety, L., Long, B., Desrosiers, G., Crémer, J.F., Locat, J., 2000. Quantification des structures biogènes en fonction d'un gradient de perturbation dans la Baie des Ha! Ha! à l'aide de la tomodensitométrie axiale. Proceedings of the 53rd Canadian Geotechnical Conference, Montreal, Québec, pp. 131–135.

Pelletier, É., Deflandre, B., Nozais, C., Tita, G., Desrosiers, G., Gagné, J.-P., Mucci, A., 1999. Crue éclair de julliet 1996 dans la région du Saguenay (Québec). 2. Impacts sur les sédiments et la biote de la baie des Ha! Ha! et du Fjord du Saguenay. Can. J. Fish. Aquat. Sci. 56, 2136–2147.

Pelletier, M., 1993. Les glissements sous-marins du bras nord

du Fjord du Saguenay, aspects geomorphologiques et geotechniques, MSc. Thesis, Universté Laval, Canada, 124 pp.

Perret, D., Locat, J., Leroueil, S., 1995. Strength development with burial in fine-grained sediments from the Saguenay Fjord, Quebec. Can. Geotech. J. 32, 247–262.

Richardson, M.D., Young, D.K., Ray, R.I., 1983. Effects of hydrodynamic and biological processes on sediment geoacoustic properties in Long Island Sound, USA. Mar. Geol. 52, 201–226.

Schaffer, C.T., Smith, J.N., 1987. Hypothesis for a submarine landslide and cohesionless sediment flows resulting from a 17th century earthquake-triggered landslide in Quebec, Canada. Geo-Mar. Lett. 7, 31–37.

Schmitt, T., Locat, J., Kammerer, E., Hill, P., Long, B., Hughes Clarke J.H., Urgeles, R., 2000. Analysis of the evolution of the reflectivity of sediments settled during the 1996 flood in the Saguenay Fjord, using the SIMRAD EM1000 multibeam sonar. Proceedings of the Canadian Hydrographic Conference 2000, Montreal, Canada, CD-ROM.

Smith, W.H.F., Wessel, P., 1990. Gridding with continuous curvature splines in tension. Geophysics 55, 293–305.

Stanic, S., Briggs, K.B., Fleischer, P., Sawyer, W.B., Ray, R.I., 1989. High-frequency acoustic backscattering from a coarse shell ocean bottom. J. Acoust. Soc. Am. 85, 125–136.

St-Onge, G., Hillaire-Marcel, C., 2001. Isotopic constraints of sedimentary inputs and organic carbon burial rates in the Saguenay Fjord, Quebec. Mar. Geol. 176, 1–22.

Stewart, W.K., Chu, D., Malik, S., Lerner, S., Singh, H., 1994. Quantitative seafloor characterization using a bathymetric sidescan sonar. IEEE J. Oceanic Eng. 19, 599–610.

Syvitski, J.P.M., Praeg, D.B., 1989. Quaternary sedimentation in the St. Laurent estuary and adjoining areas, Eastern Canada: an overview based on high-resolution seismo-stratigraphy. Géogr. Phys. Quat. 43, 291–310.

Tuttle, M., Law, K.T., Seeber, L., Jacob, K., 1990. Liquefaction and ground failure induced by the 1988 Saguenay, Quebec, earthquake. Can. Geotech. J. 27, 580–589.

Urick, R.J., 1975. Principles of Underwater Sound. McGraw Hill, New York, USA, 384 pp.

Wessel, P., Smith, W.H.F., 1991. Free software helps map and display data. EOS Trans. AGU 72, 441.

Wessel, P., Smith, W.H.F., 1998. New, improved version of the Generic Mapping Tools released. EOS Trans. AGU 79, 579.